

## Superionic Conduction in Substoichiometric LiAl Alloy: An *Ab Initio* Study

Clotilde S. Cucinotta,<sup>1,\*</sup> Giacomo Miceli,<sup>1</sup> Paolo Raiteri,<sup>1,†</sup> Matthias Krack,<sup>1,‡</sup> Thomas D. Kühne,<sup>1</sup>  
Marco Bernasconi,<sup>2</sup> and Michele Parrinello<sup>1</sup>

<sup>1</sup>Computational Science Department of Chemistry and Applied Biosciences, ETH Zurich, USI-Campus,  
Via Giuseppe Buffi 13, LUI CH-6900 Lugano

<sup>2</sup>Dipartimento di Scienza dei Materiali, Università di Milano-Bicocca, Via R. Cozzi 53, I-20125, Milano, Italy  
(Received 25 November 2008; revised manuscript received 19 June 2009; published 18 September 2009)

Based on the new *ab initio* molecular dynamics method by Kühne *et al.* [Phys. Rev. Lett. **98**, 066401 (2007)], we studied the mechanism of superionic conduction in substoichiometric Li-poor  $\text{Li}_{1+x}\text{Al}$  alloys by performing simulations at different temperatures for an overall simulation time of about 1 ns. The dynamical simulations revealed the microscopic path for the diffusion of Li vacancies. The calculated activation energy (0.11 eV) and the prefactor ( $D_0 = 6.9 \times 10^{-4} \text{ cm}^2/\text{s}$ ) for Li diffusivity via a vacancy-mediated mechanism are in good agreement with experimental NMR data. The calculation of the formation energies of different defects—Li and Al Frenkel pair and Li antisites—revealed that only  $\text{Li}^+$  vacancies and  $\text{Li}_{\text{Al}}$  antisites are present in the stability range of the Zintl phase  $-0.1 < x < 0.2$ .

DOI: 10.1103/PhysRevLett.103.125901

PACS numbers: 66.30.H-, 61.72.J-, 66.30.Fq, 71.15.Pd

The intermetallic compound  $\text{Li}_{1+x}\text{Al}$  is of interest for several aspects. It is the product of the decomposition reaction of lithium alanates which is of interest for hydrogen storage [1]. It was also proposed as an anodic material for solid state batteries [2].  $\text{Li}_{1+x}\text{Al}$  at compositions  $-0.1 < x < 0.2$  crystallizes in the *B32* structure [3,4] which corresponds to a Zintl [5] phase. As shown by electronic structure calculations, [6] an almost complete charge transfer from Li to Al takes place, leading to the formation of an Al diamond sublattice in a  $sp^3$  like electronic configuration, interpenetrated by a diamond sublattice of  $\text{Li}^+$  ions. For  $x < -0.1$  phase transitions into the  $\text{Li}_2$  phase and then into a fcc solid solution occurs. Diffusion in these latter fcc-based Al-Li alloys are mediated by vacancies and have been recently studied by *ab initio* calculations [7]. Lithium deficiency introduces  $\text{Li}^+$  vacancies ( $V_{\text{Li}}$ ) also in the *B32* phase structure while Li excess introduces  $\text{Li}_{\text{Al}}$  antisite defects, the presence of  $\text{Al}_{\text{Li}}$  antisites and Al vacancies being excluded by NMR measurements [8]. Vacancies and antisites are believed to control the superionic properties of *B32* as well. Electrochemical measurements [9] of the Li chemical diffusion coefficient reveal that Li diffusivity ( $D$ ) is weakly dependent on composition for  $x > 0$  (Li excess), while it raises steeply by decreasing the Li content ( $x < 0$ ) down to the stability boundary  $\text{Li}_{0.88}\text{Al}$ , where the activation energy is as low as 78 meV [9]. Li diffusivity at 688 K is  $\sim 3.0 \times 10^{-7} \text{ cm}^2/\text{s}$  for Li-rich alloys ( $x = 0.15$ ) and  $\sim 1.6 \times 10^{-6} \text{ cm}^2/\text{s}$  for  $\text{Li}_{0.88}\text{Al}$ . [9] NMR measurements at lower temperature (297–478 K) provide values for Li diffusivity similar to the electrochemical results and activation energies in the range 0.113–0.145 eV for the stoichiometric compound [8].

In order to provide a microscopic understanding of the superionic properties of the *B32* phase of the  $\text{Li}_{1+x}\text{Al}$  alloy,

we report here an *ab initio* simulation of the energetics and mobility of vacancies in  $\text{Li}_{1+x}\text{Al}$  alloys for  $x < -0.0156$  (Li-poor alloys) where the concentration of antisites is negligible [10]. To this aim we have adopted a new *ab initio* molecular dynamics technique, recently introduced by Kühne *et al.* [11], which allows for substantial speed up with respect to traditional Born-Oppenheimer or Car-Parrinello simulations. By means of this methodological advance, we have performed molecular dynamics simulations of a 128-atoms supercell at different temperatures for an overall simulation time of 1 ns. Such a long simulation time allows obtaining dynamical correlation factors and frequency prefactors for the diffusivity directly from the atomic trajectories at different temperatures. This direct approach enlarges the scope of *ab initio* studies of atomic diffusion in solids customarily limited to kinetic Monte Carlo simulations based on *ab initio* hopping rates computed within the transition state theory (TST). In the spirit of Car-Parrinello [12] (*CP*) approach the wave functions are not self consistently optimized during the dynamics in the scheme of Ref. [11]. However, in contrast to *CP*, large integration time steps can be used in the simulations. This scheme leads to a slightly dissipative dynamics of the type  $-\gamma_D \dot{R}_i$ , where  $R_i$  are the ionic coordinates. In Ref. [11] it was shown how to compensate this dissipation and obtain a correct canonical sampling. It has also been demonstrated that, for sufficiently small value of  $\gamma_D$ , correct dynamical properties can be obtained as well. This scheme, referred to as *CP-like* dynamics, has been implemented in the CP2K suite of programs. [13,14] We have performed spin unrestricted calculations with gradient corrected PBE exchange and correlation functional [15] and Goedecker-type [16,17] pseudopotentials. In the case of Li, the core states have been treated explicitly, while for Al, only the three valence electrons have been considered.

Kohn-Sham (KS) orbitals have been expanded in a valence DZVP Gaussian-type basis set. The charge density is expanded in a plane waves basis set with density cutoff of 400 Ry. Extension of the basis set to TZVP produces negligible change (0.1%) in the lattice parameter of LiAl. Only the  $\Gamma$ -point has been included in the Brillouin zone (BZ) integration. We have performed simulations at the four different temperatures 280 K (391 ps), 413 K (194 ps), 533 K (280 ps), and 667 K (161 ps). Values of  $\gamma_D$  in the range  $8.5 - 3.2 \times 10^{-4} \text{ fs}^{-1}$  have been used. Tests with Monkhorst-Pack (MP)  $k$  points meshes have been performed using norm conserving pseudopotentials and a plane waves expansion of the KS orbitals (35 Ry cut-off), by using the quantum-ESPRESSO package [18].

We have first studied vacancy diffusion by removing one Li atom from a 128 atom cubic supercell ( $x = -0.016$ , 49.6% Li) at the theoretical lattice constant of 6.406 Å. The tetrahedral cage of Li atoms around the vacancy shrinks inward. At the simulation temperatures, the average Li-Li distance along the cage edges is as small as 3.8 Å, to be compared with the value of 4.5 Å, in the perfect crystal. At all temperatures the vacancy diffuses very fast, doing on average 1.95, 2.18, 2.80 and 3.44 single jumps per ps, at 280, 413, 533, and 667 K, respectively. In the observed vacancy diffusion mechanism, the jump of a neighboring Li atom in the vacancy site is accompanied by the asymmetric expansion (contraction) of the tetrahedral cage around the initial (final) vacancy position. As an extra test, 20 ps of Born-Oppenheimer molecular dynamics at 400 K in a 432 atoms cell, with two vacancies ( $x = -0.010$ , 49.76% Li) has been conducted, showing that the vacancies diffuse independently, with the same mechanism observed in the smaller cell. No competing mechanism arise at high temperature (667 K). The Li tracer diffusivity  $D_{\text{Li}}^*$  is obtained directly from the Li mean square displacement as  $\langle x_{\text{Li}}(t)^2 \rangle_{t \rightarrow \infty} = 6tD_{\text{Li}}^*$ . The tracer diffusivity  $D_{\text{Li}}^*$  is well described by an Arrhenius plot with an activation energy of 34 meV in the temperature range investigated (see inset of Fig. 1). The tracer diffusivity is related to the average residence time  $\tau_{\text{vac}}$  of the vacancy in its site by

$$(1 - c_{\text{vac}})D_{\text{Li}}^* = f_c c_{\text{vac}} \frac{a^2}{6\tau_{\text{vac}}} = f_c c_{\text{vac}} D_{\text{vac}}, \quad (1)$$

where  $a$  is the interatomic Li-Li distance in the perfect crystal (2.774 Å),  $c_{\text{vac}}$  is the vacancy concentration and  $f_c$  is a correlation factor which contains information on correlations between individual jumps of Li atoms [19].  $f_c$  is equal to 0.5 for vacancy-mediated diffusion in a diamond sublattice and in the lack of any further dynamical correlation among the Li jumps (e.g., due to vacancy-vacancy interactions or enhanced forward-backward jumps not contributing to diffusivity). In general, to assess possible deviation of  $f_c$  from the ideal value, substantially longer simulation times are needed than those required to estimate

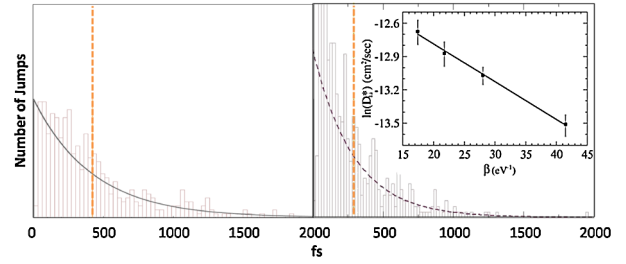


FIG. 1 (color online). Normalized jump-times distribution for the vacancy, as obtained from 194 ps  $CP$ -like dynamics at 412 K (453 jump events) and at 667 K (553 jumps). The distribution is fitted with an exponential function  $\frac{1}{\tau_{\text{vac}}} \exp(-\frac{t}{\tau_{\text{vac}}})$  where  $\tau_{\text{vac}} = 425$  fs and 291 fs for 412 and 667 K, respectively, the vertical lines represent the mean jump times for the vacancy. From 0 to 30 fs, the distribution deviates from the exponential behavior, this interval representing the relaxation time of the vacancy in its site. In the inset, the Arrhenius plot of the tracer diffusion coefficient  $D_{\text{Li}}^*$  as a function of  $\beta = (k_B T)^{-1}$  (in  $\text{eV}^{-1}$ ).

the tracer diffusivity. As shown in Fig. 1, the distribution of the residence times of the vacancy in its site is well described by an exponential function  $\frac{1}{\tau_{\text{vac}}} \exp(-\frac{t}{\tau_{\text{vac}}})$ .

By plugging in Eq. (1) the calculated values for  $\tau$  and  $D_{\text{Li}}^*$  ( $c_{\text{vac}} = \frac{1}{64}$ ) we obtain  $f_c = 0.45$  for the three highest temperatures, which is still very close, considering our uncertainties, to the ideal value of 0.50 for vacancy-mediated diffusion in a diamond sublattice. However,  $f_c$  turns out to be as small as 0.34 at the lowest temperature (280 K) which indicates the presence of further correlations in the Li motion. The analysis of the trajectories revealed that this is due to the presence of correlated jumps of the vacancy in the form of forward-backward jumps which do not contribute to the diffusivity. The probability for the vacancy to come back in its previous site is as large as 0.4 at 280 K, to be compared with the ideal value of 0.25 for an uncorrelated Brownian motion of the single vacancy on a diamond lattice. The enhanced probability for a vacancy to come back in its previous position is probably due to the fact that at the lowest temperatures the cage of Li atoms around the initial and final position does not relax sufficiently fast to make subsequent jumps fully uncorrelated.

The Arrhenius fit of  $D_{\text{Li}}^*$  (inset of Fig. 1) yields a vacancy diffusivity  $D_{\text{vac}}$  as defined by Eq. (1) of  $D_{\text{vac}} = D_0 \exp(-\frac{\Delta E}{k_B T})$  with the prefactor  $D_0 = 6.9 \times 10^{-4} \text{ cm}^2/\text{s}$ . This results in  $D_{\text{vac}} \sim 3.6 \times 10^{-4} \text{ cm}^2/\text{s}$  at 600 K which is sizably larger than the calculated value of  $D_{\text{vac}} \sim 10^{-6} \text{ cm}^2/\text{s}$  for fcc  $\text{Al}_{1-x}\text{Li}_x$  solid solution (with  $x < 0.15$ ) at the same temperature [7]. Indeed in the  $B32$  phase the vacancy diffuses only in the sublattice of the more mobile Li atoms. NMR measurements at low temperature (297–478 K) provide the prefactor  $D_0$  for single vacancy diffusivity in the range  $4.4\text{--}7.2 \times 10^{-4} \text{ cm}^2/\text{s}$  (for  $x = -0.066\text{--}0$ ) [8,20] which is very close to our result consid-

ering the theoretical uncertainties and the large spread in measured values. Concerning the activation energy, NMR measurements of  $^7\text{Li}$  spin-lattice relaxation at  $x = -0.066$  yield values in the range 0.128–0.145 eV [8,10,20–22], while electrochemical measurements yields an activation energy for Li diffusion of 78 meV at  $x \sim -0.1$  [9].

To assess possible inaccuracy in the our estimated activation energy, we have performed zero temperature optimization of the minimum energy path (MEP), assuming the mechanism identified in the dynamical simulation. We have used the nudged-elastic band [23,24] (NEB) method and the same 128-atoms supercell used in the dynamical simulation. By restricting the BZ integration to the supercell  $\Gamma$ -point, the activation energy for diffusion turns out to be equal (within 3 meV) to the value of 34 meV extracted from the dynamical simulation. The transition state (TS) is a single saddle point as demonstrated by the calculation of the Hessian matrix (computed by finite differences and by still sampling the BZ at the  $\Gamma$  point). From phonon frequencies at the TS and at the initial configuration, we have estimated the prefactor  $D_0$  within the harmonic approximation to TST. The resulting  $D_0$  is 30 times larger than the value inferred from the dynamical simulations. This discrepancy might be ascribed to frequent recrossing events (neglected within TST) in the presence of a relatively flat saddle point (cf. Fig. 2) which might also be responsible for the correlated vacancy jumps at low temperature (280 K) mentioned above. The dynamical simulations seem thus mandatory to obtain the correct order of magnitude for the

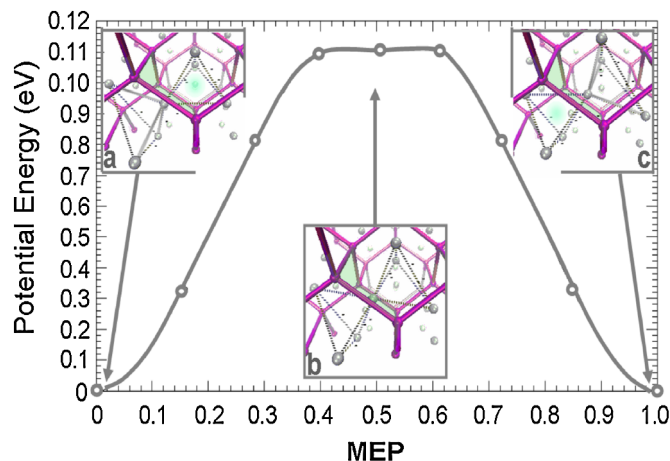


FIG. 2 (color online). Potential energy surface along the MEP for vacancy diffusion. In the insets, the initial (a), transition (b) and final (c) configurations of the MEP for vacancy migration between two neighboring sites. The vacancy indicated by a light-green spot is at the center of the Li tetrahedron on the right (left) in panel (c) [(a)]. At transition state (b), the two distorted tetrahedra are symmetric with respect to the  $\text{Li}^+$  ion at the common vertex involved in the diffusion process. This latter passes through the center of the shadowed (in green) hexagonal-chair ring of Al atoms. Li atoms are represented in white. Al atoms are represented in dark violet and are connected by bonds.

frequency prefactor in this system. By refining the BZ integration over a  $3 \times 3 \times 3$  MP mesh the path does not change sizably but the activation energy raises up to 0.11 eV, which is in better agreement with the experimental data. The potential energy along the MEP, the geometry of the initial, final and transition states are shown in Fig. 2. A plot of the charge density at the TS is given as additional material. In view of the very good agreement with experiments, our results point to the conclusion that in Li-poor alloys at temperature below 700 K,  $\text{Li}^+$  diffusion occurs through simple vacancy jumps.

As a further check of the internal consistency of our picture we have explored whether, in the Li-poor region, excess vacancies might also be produced in sizeable amount via thermally generated Li Frenkel pairs. To this aim we have calculated the formation energy of a Frenkel pair [25] ( $\text{Li}_{\text{int}}$  and  $V_{\text{Li}}$  as far as possible) in the 128-atoms cell which turned out to be  $E_f = 1.94$  eV. Assuming an Arrhenius behavior, this corresponds to a vacancy concentration of  $\sim 10^{-7}$  at 688 K, which is several order of magnitude lower than that of constitutional vacancies due to defects in stoichiometry. The formation energy of an Al Frenkel pair is instead as large as 3.10 eV. In this respect we note that a pair of Li and Al vacancies is unstable with respect to the formation of two  $\text{Li}_{\text{vac}}$  and a  $\text{Li}_{\text{Al}}$  antisite. In fact, the energy that is gained when a Li atom is moved into a Al vacancy is 0.38 eV, as it results from calculating the energy difference between these two configurations, in a 128 atoms supercell. This explains why Al vacancies and interstitials are not to be found in LiAl alloys [22]. On the other hand, the insertion of two  $\text{Li}_{\text{vac}}$  and one  $\text{Li}_{\text{Al}}$  in a perfect stoichiometric 128 atoms cell leads to a slightly negative formation energy ( $-65$  meV), which indicates that at low defects concentration these defects form spontaneously. This result is consistent with the experimental estimate of defects concentration obtained from the variation of lattice parameters as a function of composition. These data have been modeled indeed by assuming that additional  $V_{\text{Li}}$  and  $\text{Li}_{\text{Al}}$  defects in proportion 2:1 can be introduced without changing the stoichiometry. It turns out that at  $x = 0$  the concentration of defects is as large as 3.6%  $V_{\text{Li}}$  and 1.8%  $\text{Li}_{\text{Al}}$  in the corresponding sublattice [10]. The concentration of  $\text{Li}_{\text{Al}}$  decreases rapidly by decreasing  $x$  and vanishes at the phase boundary  $x = -0.12$ , while a large concentration of  $V_{\text{Li}}$  is still present in Li-rich alloys amounting at 0.4% for  $x = 0.15$  [10]. In our calculations, an increase in the defects concentration from the addition of another pair of  $\text{Li}_{\text{vac}}$  and one  $\text{Li}_{\text{Al}}$  (which corresponds to  $c_{\text{vac}} = 0.062$  and  $c_{\text{anti}} = 0.031$ ) leads to a positive value of 0.48 which indicates that the theoretical equilibrium value of  $c_{\text{vac}}$  is between 0.031 and 0.062 to be compared with the experimental value 0.036 [10,26]. Because of the small size of our simulation cells, a more compelling comparison with the measured  $c_{\text{vac}}$  [10] is unfortunately not possible since the defect concentration

can only be varied by discrete values in our small simulation cell.

To reconcile the low value of  $D$  for  $x > 0$  and the high concentration of vacancies inferred from the density measurements an attractive interaction between  $V_{\text{Li}}$  and  $\text{Li}_{\text{Al}}$  which reduces the mobility of  $V_{\text{Li}}$  has been postulated in literature [8]. We do not find evidence for the proposed [8,10] formation of a  $V_{\text{Li}}$  and  $\text{Li}_{\text{Al}}$  bound complex, instead, these defects slightly repel each other. In fact, the configuration with the two defects as far as possible in the 128-atoms cell is 0.16 eV lower in energy with respect to the configuration with the two defects in nearest neighbor positions [27]. This repulsion, however, will also affect vacancy diffusivity due to possible reduction in the number of low energy percolating paths induced by the increase of antisite defects [28].

In summary, based on a new *ab initio* molecular dynamics method [11], we have studied the microscopic mechanism of  $\text{Li}^+$  diffusivity in substoichiometric Li-poor  $\text{Li}_{1+x}\text{Al}$  alloys by performing simulations at different temperatures for an overall simulation time of about 1 ns. The calculated activation energy and prefactor for a single vacancy diffusion obtained by an Arrhenius plot are in very good agreement with experimental data which demonstrate that diffusion in Li-poor alloys is due essentially to the uncorrelated motion of stoichiometric vacancies. Although the modeling of the Li-rich region is outside the scope of the present work, our results on the energetics of vacancies and antisite support the conjecture that ionic mobility in Li-rich alloys might instead be determined by a complex interplay between defects.

We gratefully thank R. Car for discussion and information. M. Ceriotti and P. Elvati are also acknowledged for support and discussion. The authors are also grateful to M. Valle (CSCS) for his help with visualization. This work was supported by a grant from the Swiss National Supercomputing Centre-CSCS, under project ID s206.

\*Corresponding author.

c.cucinotta@phys.chem.ethz.ch

†Present address: Nanochemistry Research Institute, Department of Chemistry, Curtin University of Technology, GPO Box U1987, Perth, Western Australia 6845.

‡Present address: Paul Scherrer Institute, 5232 Villigen PSI, Switzerland.

- [1] J. K. Kang, J. Y. Lee, R. P. Muller, and W. A. Goddard, III, *J. Chem. Phys.* **121**, 10 623 (2004).
- [2] J. M. Tarascon and M. Armand, *Nature (London)* **414**, 359 (2001).
- [3] H. Ehrenberg, H. Pauly, M. Knapp, J. Gröbner, and D. Mirkovic, *J. Solid State Chem.* **177**, 227 (2004).
- [4] K. M. Myles, F. C. Mrazek, J. A. Smaga, and J. L. Settle, in *Proceedings of the Symposium and Workshop on Advanced Battery Research and Design*, U.S. ERDA Report, ANL 76-8, B-50, Argonne National Laboratory, 1976.
- [5] E. Zintl and G. Brauer, *Z. Phys. Chem. B* **20**, 245 (1933).
- [6] X. Q. Guo, R. Podloucky, and A. J. Freeman, *Phys. Rev. B* **40**, 2793 (1989).
- [7] A. Van der Ven and G. Ceder, *Phys. Rev. Lett.* **94**, 045901 (2005).
- [8] S. C. Chen, J. C. Tarczon, W. P. Halperin, and J. O. Brittain, *J. Phys. Chem. Solids* **46**, 895 (1985).
- [9] C. J. Wen, B. A. Boukamp, R. A. Huggins, and W. Weppner, *J. Electrochem. Soc.* **126**, 2258 (1979).
- [10] K. Kishio and J. O. Brittain, *J. Phys. Chem. Solids* **40**, 933 (1979).
- [11] T. D. Kühne, M. Krack, F. R. Mohamed, and M. Parrinello, *Phys. Rev. Lett.* **98**, 066401 (2007).
- [12] R. Car and M. Parrinello, *Phys. Rev. Lett.* **55**, 2471 (1985).
- [13] J. VandeVondele, M. Krack, F. Mohamed, M. Parrinello, T. Chassaing, and J. Hutter, *Comput. Phys. Commun.* **167**, 103 (2005).
- [14] CP2K suite of programs; see: <http://cp2k.berlios.de/>.
- [15] J. P. Perdew, K. Burke, and M. Ernzerhof, *Phys. Rev. Lett.* **77**, 3865 (1996).
- [16] S. Goedecker, M. Teter, and J. Hutter, *Phys. Rev. B* **54**, 1703 (1996).
- [17] M. Krack, *Theor. Chem. Acc.* **114**, 145 (2005).
- [18] S. Baroni *et al.* (2007); <http://www.quantum-esspresso.org> and <http://www.pwscf.org>.
- [19] G. E. Murch, *Solid State Ionics* **7**, 177 (1982).
- [20] T. Asai, M. Hiratani, and S. Kawai, *Solid State Commun.* **53**, 55 (1985).
- [21] T. Tokuhito, S. Susman, T. O. Brun, and K. Violin, *J. Phys. Soc. Jpn.* **58**, 2553 (1989).
- [22] J. R. Willhite, N. Karnezos, P. Cristea, and J. O. Brittain, *J. Phys. Chem. Solids* **37**, 1073 (1976).
- [23] G. Henkelman and H. Jónsson, *J. Chem. Phys.* **113**, 9978 (2000).
- [24] G. Henkelman, G. Johannesson, and H. Jónsson, *Methods for Finding Saddle Points and Minimum Energy Paths in Progress on Theoretical Chemistry and Physics* (Kluwer Academic, New York, 2000).
- [25] See EPAPS Document No. E-PRLTAO-103-019940 for the description of the effect of  $k$  points sampling on the geometry of  $V_{\text{Li}}$ , for the interaction energy of  $\text{Li}_{\text{Al}}$  and  $V_{\text{Li}}$  as a function of their distance and for the charge density at the transition state on the (110) and (111) planes. This document can be reached through a direct link in the on-line article's HTML reference section or via the EPAPS home page (<http://www.aip.org/pubservs/epaps.html>).
- [26] At even higher defect concentration ( $c_{\text{vac}} = 0.094$  and  $c_{\text{anti}} = 0.047$ , modeled inserting three pairs of  $\text{Li}_{\text{vac}}$  and three  $\text{Li}_{\text{Al}}$  in a 128-atoms supercell) the formation energy is very similar (0.50 eV).
- [27] Our simulations also show that the two vacancies repel each other, the configuration with two vacancies as far as possible within our cell gaining 90 meV with respect to the configuration with the two vacancies nearest neighbors.
- [28] Simulations at 680 K (15 ps long) of a 128-atoms cell with an Al antisite have not shown diffusion of Li from the antisite position.